Towards CFD-Based Aeroelastic Analysis of NLF Wings

Sebastian Helm(✉), Michael Fehrs, and Jens Nitzsche

DLR, Institute of Aeroelasticity, 37073 Göttingen, Germany
sebastian.helm@dlr.de
https://www.dlr.de/ae/

Abstract. The effect of Natural Laminar Flow (NLF) on the aeroelastic behavior of transport aircraft wings is widely unknown. This numerical study investigates the influence of boundary layer transition on the unsteady aerodynamic response of an NLF test case, the DLR-F5 wing. State-of-the-art RANS methods for transition prediction are compared at wind tunnel and free-flight conditions. A more critical flutter behavior is indicated in the case of transitional flow.

Keywords: Natural laminar flow · Aeroelasticity · Flutter

1 Introduction

Laminar wing technology has the potential to reduce aircraft drag significantly. However, the impact on the aeroelastic behavior (e.g. the flutter boundary) of natural laminar flow wings is still widely unknown and subject to ongoing discussion [1]. The reduced displacement thickness of a transitional boundary layer alters the aerodynamic forces even at flight Reynolds numbers [2]. In particular, the strength and position of recompression shocks differ considerably from a fully turbulent boundary layer flow. The unsteady airloads determine the dynamic aeroelastic behavior and can be expected to inherit these effects. Experimental and numerical analyses of NLF airfoils in transonic flow at low Reynolds numbers show a reduction of the flutter stability due to the influence of partially laminar flow [3,4]. To the authors knowledge, no similar investigations exist for NLF wings at high Reynolds numbers. The objective of the present research is to fill this gap and attain the capability to perform a flutter analysis of an NLF wing taking the effect of laminar-turbulent transition into account. This paper gives some insight into the CFD-based aerodynamics of NLF wings with state-of-the-art transition models.

2 Simulation Set-Up

The TAU transition module (involving the linear stability code LILO and the e^N method [5,6]), the γ-Re_θ transition model [7,8], and the γ transition model

A. Dillmann et al. (Eds.): DGLR 2018, NNFM 142, pp. 491–500, 2020.
https://doi.org/10.1007/978-3-030-25253-3_47

[2] are used for transition prediction in RANS simulations with the DLR TAU-Code. The SST $k-\omega$ turbulence model of Menter [9] is applied for fully turbulent computations and for the turbulent part of the transitional flow. The unsteady aerodynamics are computed by linear system identification based on the response to small-amplitude pulse excitation [10].

3 Test Case

The DLR-F5 wing (also known as DFVLR-F5) is designed to provide experimental data for validation of computational aerodynamics. The 20°-swept wing with an aspect ratio $AR \equiv b^2/S = 9.5$ allows a large amount of 2D flow [13]. Because of the planform and the shock-free design condition of the airfoil at $M = 0.78$, it is considered representative for an NLF transport aircraft, even though the wing is symmetric. The section at 77% wing span is shown in Fig. 1. At its root, the wing blends smoothly from the analytically defined airfoil into the side wall, which is effectively a splitter plate to obtain a well-defined boundary layer [14].

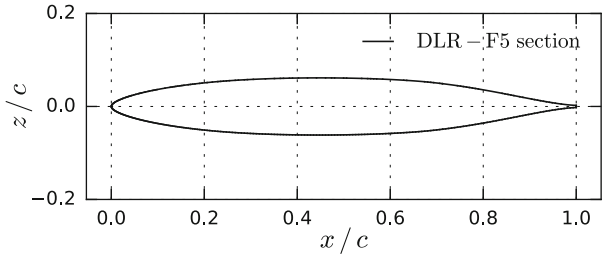

Fig. 1. DLR-F5 airfoil geometry (wing section at $\eta = 0.77$)

The DLR-F5 wing model with $c_{mac} = 0.15$ m is tested in the DNW-TWG (Transonic Wind Tunnel Göttingen) at $\alpha = 0°$ and 2°, $M = 0.82$, $Re_{mac} = 1.5 \cdot 10^6$ [13]. A turbulence level of $Tu = 0.35\%$ is assumed. Laminar-turbulent transition is free. Therefore, the DLR-F5 wing has become a standard test case. It was already used for validation of the γ-Re_θ transition model [11,12].

4 Validation

The computational grid consists of approximately $13{\cdot}10^6$ nodes. A spherical CFD domain with a radius of 100 m is used. A no-slip boundary condition is imposed on the splitter plate defined by the control volume geometry given by Sobieczky [15]. The boundary layer flow on the splitter plate is tripped numerically by defining an arbitrary low transition onset Reynolds number at the leading edge of the plate. The boundary layer grid on the upper and lower wing side consists of 330 nodes in span direction and 200 nodes in chord direction with. 75 prism

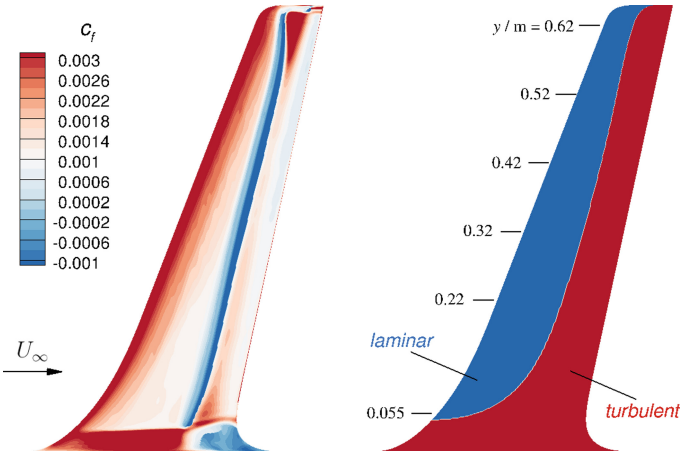

Fig. 2. Skin friction coefficients predicted numerically using the γ model (left) and experimental transition location (right) on the upper surface of the DLR-F5 wing, $\alpha = 2°$

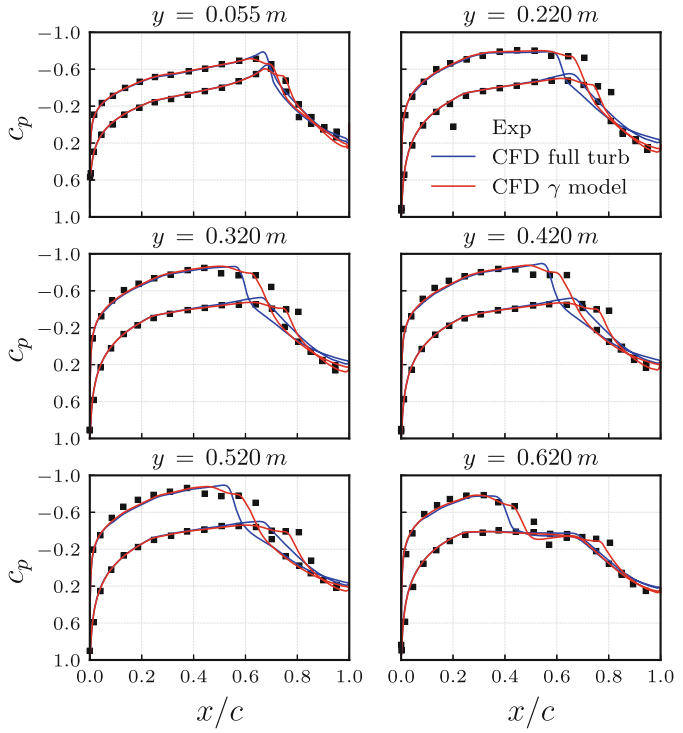

Fig. 3. Pressure distributions in spanwise sections, $\alpha = 2°$

layers were used. Unstructured surface grid are used for wing tip and splitter plate. The maximum y^+ value is below one throughout this investigation.

The skin friction distribution on the upper wing surface predicted numerically using the γ model is shown in Fig. 2. In addition, the experimental transition location given by Sobieczky [13] is depicted on the right. The attachment line transition originating from the turbulent boundary layer flow on the splitter plate is captured by the computation. However, the spanwise extent is too small and there is no smooth variation of the transition location from the wing root in span direction. Laminar flow over 50 to 60% of the chord is achieved at mid-wing before transition takes place above a laminar separation bubble preceding the recompression shock.

A comparison of experimental and numerical pressure distributions in several spanwise sections is shown in Fig. 3. Over the most part of the wing span, the shock position in the transitional computation is about 5% of the chord further downstream, compared to the fully turbulent case. Furthermore, laminar separation occurs in the case of transitional flow. The size of the separation bubble is underestimated. It is important to note, that the partially laminar flow has a considerable influence on the steady aerodynamics in transonic flow. The prediction of steady pressure distributions is significantly improved when transition is taken into account.

5 Results

5.1 2D Wind Tunnel Conditions

The wing section at $y = 0.5$ m ($\eta = 0.77$, Fig. 1) of the DLR-F5 wing is used for 2D analysis. The computational grid contains 300 nodes in chord direction and 100 structured layers in wall-normal direction to resolve the boundary layer. Flow conditions corresponding to the wind tunnel case of the previous section are investigated ($Ma = 0.78$, $Re = 1.5 \cdot 10^6$, $Tu = 0.35\%$). The steady lift, drag and moment curves are shown in Fig. 4. Transitional cases show a steeper lift curve slope $dc_l/d\alpha$ for the most part up to $\alpha \approx 1.5°$. This increase is caused by the boundary layer effect on the effective airfoil shape. According to Bendiksen [16], a steeper lift curve indicates the reduction of flutter stability occurring in the transonic domain, known as transonic dip. Furthermore, a lower (more negative) moment curve slope is an indicator for the possibility of single-degree-of-freedom flutter.

At the present flow conditions, the methods available for transition prediction yield similar results in terms of transition location, drag benefit and extent of the drag bucket. It is observed that the e^N method does not converge for angles of attack $\alpha > 1.3°$. The e^N method is omitted for the computation of unsteady aerodynamic forces as it is not well suited for pulse computations. This is because of high computational costs and the proneness to yield oscillating transition locations. Instead, a fixed transition location previously determined from steady computation is prescribed by means of the TAU transition module.

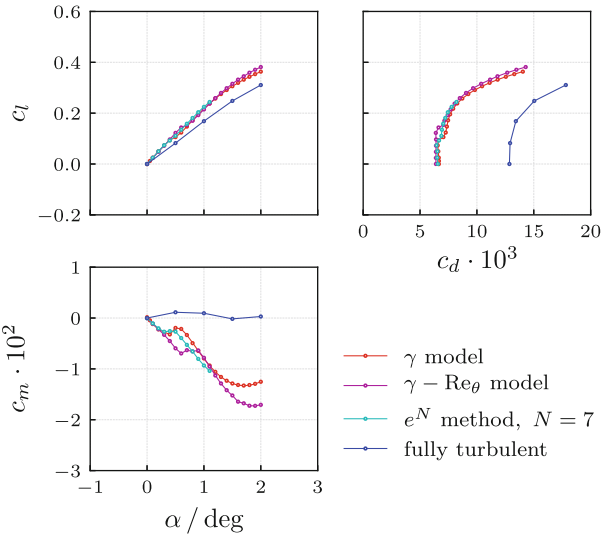

Fig. 4. 2D: steady aerodynamic coefficients at $M = 0.78$, $Re_{mac} = 1.5 \cdot 10^6$

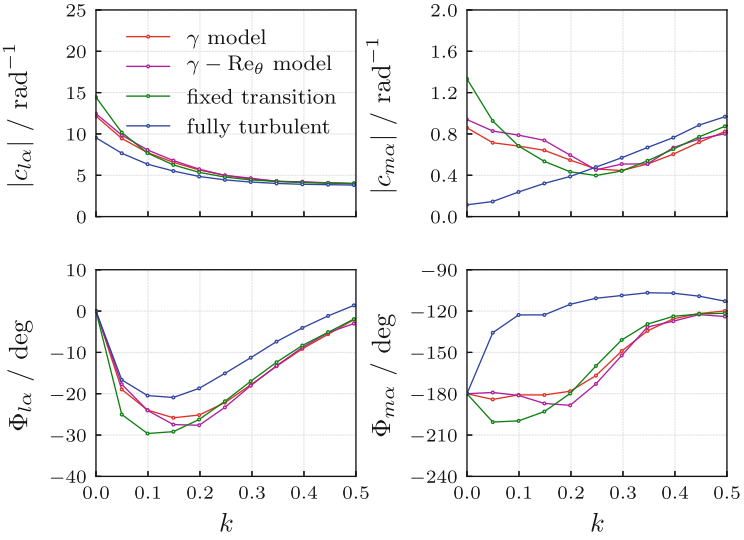

Fig. 5. 2D: unsteady aerodynamic coefficients in magnitude (top) and phase (bottom) at $\alpha_m = 1°$, $M = 0.78$, $Re_{mac} = 1.5 \cdot 10^6$

This simplified transition prescription allows no unsteady variation of the transition location in time-accurate computations, as opposed to the correlation-based transition models.

Figure 5 shows the unsteady lift and moment coefficient due to a pitch excitation at a mean angle of attack $\alpha_m = 1°$. The pulse excitation is defined by a rotational amplitude $\hat{\alpha} = 1° \cdot 10^{-3}$ about the moment reference location $(c/4)$. The unsteady aerodynamic forces are plotted in magnitude and phase with respect to the reduced frequency $k = \frac{\omega c}{2U_\infty}$. Significant differences between the fully turbulent and the transitional solutions are observed, e.g. a difference of up to 80° in the phase of the moment coefficient. With regard to aeroelastic analysis, it is important to note that the unsteady moment exhibits a phase lead in the frequency range $k < 0.2$. This is known to enable single-degree-of-freedom flutter.

5.2 2D Free-Flight Conditions

Free-flight conditions of transport aircraft involve higher Reynolds numbers and lower turbulence levels compared to the wind tunnel conditions discussed above. Therefore, computations are performed at $Re = 30 \cdot 10^6$ and $Tu = 0.05\%$ (resp. a critical N-factor $N = 9$).

The steady aerodynamic coefficients are shown in Fig. 6. The γ-Re_θ model predicts an almost fully turbulent flow as the underlying correlation is not suited for accelerated flows [2]. It is, therefore, omitted below. In contrast to that, the γ transition model gives similar results as the e^N method for $\alpha \geq 1°$. For lower angles of attack, the e^N method fails to obtain a converged transition location. Therefore, only angles of attack $\alpha \geq 1°$ are considered.

Figure 7 shows the unsteady aerodynamic coefficients due to pitch excitation about $\alpha_m = 1°$. All computations show a qualitatively similar behavior with a phase lead of the unsteady moment coefficient over a large frequency range. It is important to note, that significant differences between transitional and fully turbulent flow remain, even for the high Reynolds numbers. A similar behavior is observed by Fehrs [2] with the RAE2822 airfoil at similar (free-flight) conditions. The unsteady computations with prescribed transition location give almost identical results as the γ transition model. This could indicate that the transition model is not able to predict the unsteady transition behavior correctly, or the effect of unsteady boundary layer is small compared to other unsteady effects at high Reynolds numbers. Future experimental and numerical investigation will have to answer this question by detailed analysis.

5.3 3D Free-Flight Conditions

Free-flight flow conditions of the 3D test case are $M = 0.82$, $Re_{mac} = 30 \cdot 10^6$ and $Tu = 0.05\%$. The computational grid contains approximately $18.2 \cdot 10^6$ nodes. A symmetry boundary condition is imposed instead of the splitter plate at the wing root. The boundary layer grid on the wing consists of 300 nodes in span direction, 200 nodes in chord direction and 95 prism layers.

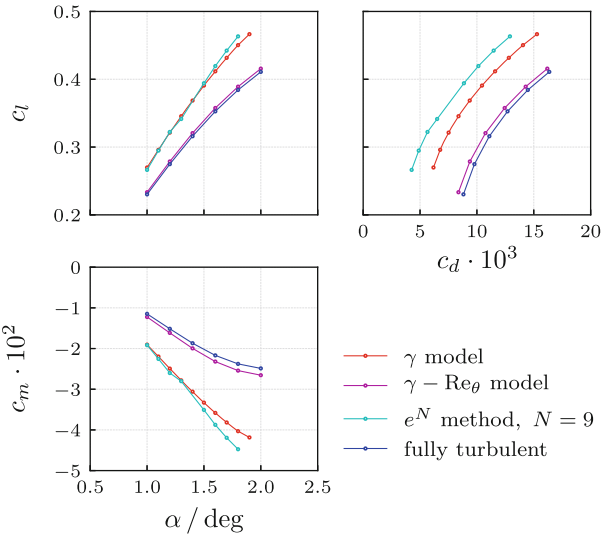

Fig. 6. 2D: steady aerodynamic coefficients at $M = 0.78$, $Re_{mac} = 30 \cdot 10^6$

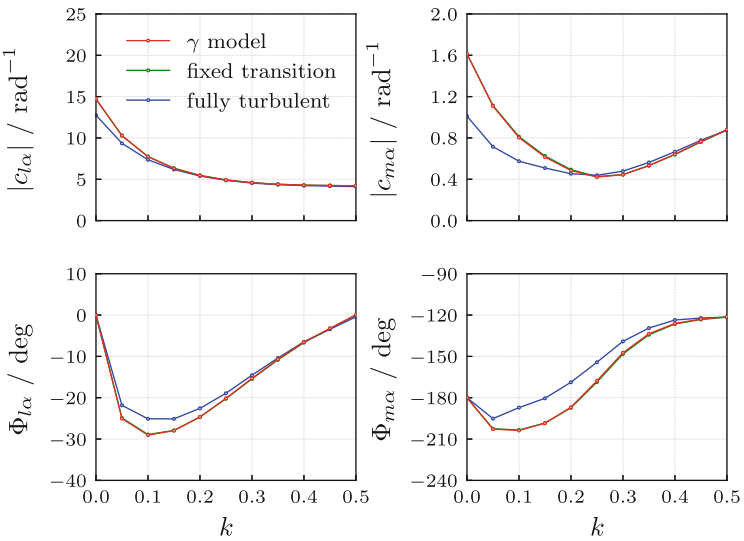

Fig. 7. 2D: unsteady aerodynamic coefficients in magnitude (top) and phase (bottom) at $\alpha_m = 1°$, $M = 0.78$, $Re_{mac} = 30 \cdot 10^6$

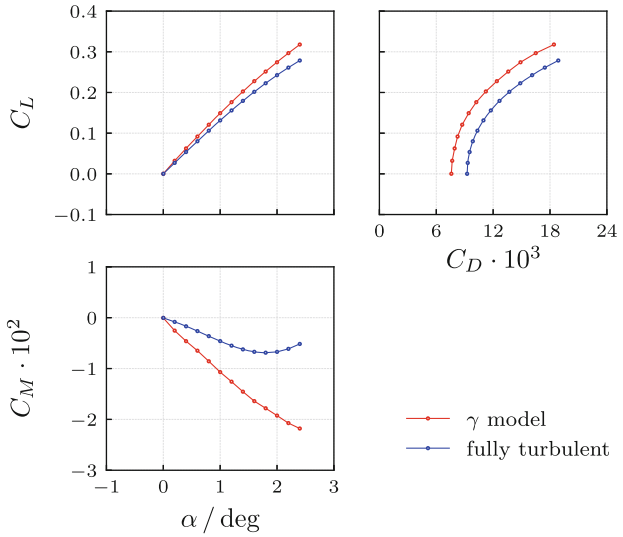

Fig. 8. 3D: aerodynamic coefficients at $M = 0.82$, $Re_{mac} = 30 \cdot 10^6$

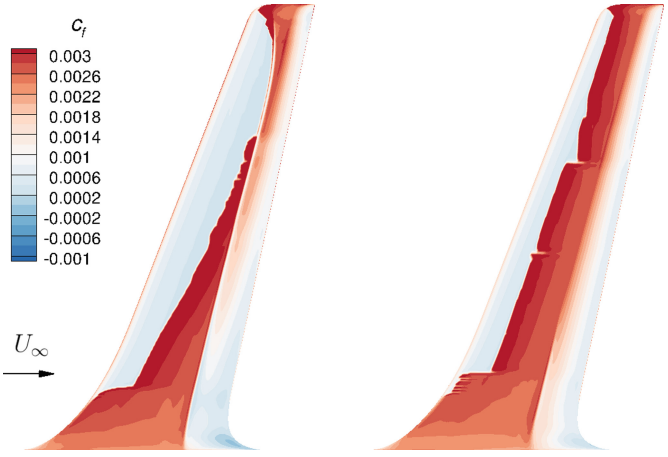

Fig. 9. 3D: skin friction coefficients on upper (left) and lower (right) surface at $\alpha = 1°$, $M = 0.82$, $Re_{mac} = 30 \cdot 10^6$, $Tu = 0.05\%$, γ model

Figure 8 shows the steady aerodynamic coefficients for the transitional and fully turbulent flow. The reference coordinate for the moment coefficient is given by the quarter-point location of the *mac*-section at 44% wing span. The transitional and fully turbulent aerodynamic lift and moment coefficients diverge for increasing angles of attack, similar to the 2D results. Therefore, we expect the unsteady aerodynamic response of the 3D wing to show similar differences (between transitional and fully turbulent flow) as the 2D airfoil section in the previous section.

The extent of laminar flow at $\alpha = 1°$ can be seen from the skin friction distribution in Fig. 9. In contrast to fully turbulent flow, there is a reverse flow region on the upper surface at the trailing edge at the wing root section.

At the moment, the unsteady aerodynamic response of the DLR-F5 wing is investigated, including spatial and temporal convergence studies. Up to now, it is found that unsteady three-dimensional flows with free boundary layer transition are more sensitive to the spatial and temporal discretization, which results in an increased pre- and post-processing effort.

6 Conclusion

The DLR-F5 wing experiment with free boundary layer transition is used for further validation of the γ transition model. Good agreement of different transition prediction methods is obtained at wind tunnel conditions. For transport aircraft flight conditions and off-design angles of attack, the γ transition model is the most robust among the methods considered. However, it gives a shorter laminar length compared to the e^N method. This indicates that the underlying correlation might need a revision.

The CFD-based analysis emphasizes the importance of boundary layer transition for the unsteady aerodynamic response of NLF airfoils and wings. Throughout the study, significant effects of laminar-turbulent transition are found, even at high Reynolds numbers. The results indicate a different flutter behavior of laminar airfoils with free boundary layer transition as considerable differences are found in the unsteady moments. Future work will further extend the scope of flight conditions systematically and include a flutter analysis. Furthermore, the influence of unsteady motion of the transition location needs to be investigated in more detail.

References

1. Tichy, L., Mai, H., Fehrs, M., Hebler, A.: Risk analysis for flutter of laminar wings. In: 17th International Forum on Aeroelasticity and Structural Dynamics, IFASD, Como, Italy (2017)
2. Fehrs, M.: Boundary layer transition in external aerodynamics and dynamic aeroelastic stability. Dissertation, Technische Universität Carolo-Wilhelmina zu Braunschweig, Braunschweig, Germany (2018). ISSN 1434-8454, ISRN DLR-FB–2018-11, also NFL-FB 2017-27

3. Fehrs, M., van Rooij, A.C.L.M., Nitzsche, J.: Influence of boundary layer transition on the flutter behavior of a supercritical airfoil. CEAS Aeronaut. J. **6**(2), 291–303 (2015)
4. Hebler, A.: Experimental assessment of the flutter stability of a laminar airfoil in transonic flow. In: 17th International Forum on Aeroelasticity and Structural Dynamics, IFASD, Como, Italy (2017)
5. Krumbein, A., Krimmelbein, N., Schrauf, G.: Automatic transition prediction in hybrid flow solver, part 1: methodology and sensitivities. J. Aircr. **46**(4), 1176–1190 (2009)
6. Krumbein, A., Krimmelbein, N., Schrauf, G.: Automatic transition prediction in hybrid flow solver, part 2: practical application. J. Aircr. **46**(4), 1191–1199 (2009)
7. Langtry, R.B., Menter, F.R.: Correlation-based transition modeling for unstructured parallelized computational fluid dynamics codes. AIAA J. **47**(12), 2894–2906 (2009)
8. Seyfert, C., Krumbein, A.: Evaluation of a correlation-based transition model and comparison with the e^N method. J. Aircr. **49**(6), 1765–1773 (2012)
9. Menter, F.R.: Two-equation eddy-viscosity turbulence models for engineering applications. AIAA J. **32**(8), 1598–1605 (1994)
10. Kaiser, C., Thormann, R., Dimitrov, D., Nitzsche, J.: Time-linearized analysis of motion-induced and gust-induced airloads with the DLR TAU Code. Deutscher Luft- und Raumfahrtkongress 2015, Rostock, Germany (2015)
11. Langtry, R.B.: A correlation-based transition model using local variables for unstructured parallelized CFD codes. Ph.D. Dissertation, University Stuttgart, Stuttgart (2006)
12. Nie, S.: Extension of transition modeling by a transport equation approach. Ph.D. Dissertation, Technische Universität Carolo-Wilhelmina zu Braunschweig, Braunschweig, Germany (2017)
13. Sobieczky, H.: DLR-F5: test wing for CFD and applied aerodynamics. In: A Selection of Experimental Test Cases for the Validation of CFD Code, AGARD-AR-303, Québec, Canada, vol. II (1994)
14. Sobieczky, H., Hefer, G., Tusche, S.: DFVLR - F5 test wing experiment for computational aerodynamics. In: 5th Applied Aerodynamics Conference, AIAA-Paper 87, Monterey, CA, USA, pp. 479–487 (1987)
15. Sobieczky, H.: DFVLR-F5 test wing configuration - the boundary value problem. In: Kordulla, W. (ed.) Notes on Numerical Fluid Mechanics, vol. 22. Vieweg, Braunschweig (1988)
16. Bendiksen, O.O.: Review of unsteady transonic aerodynamics: theory and applications. Prog. Aerosp. Sci. **47**, 135–167 (2011)